Chapter 5

Infinite 2D Plate Model

"If it runs
It good enough for me"
Bad Livers

5.1 Introduction

In previous chapters, the intent of WRC-planar models was to include dynamic interactions that inherently affected the treated system response. These interactions such as damping and mass loading affect the results of the noise control investigation. However these effects are not considered the primary noise control mechanism, i.e., source strength control by surface velocity alteration. Furthermore both models used time-consuming numerical integration as a means to investigative results.

In this chapter a new model is developed including the acoustic quantities such as pressure, intensity, and sound power for wavenumber analysis of an infinite plate (baseline) and with WRC as noise control treatment. These quantities use the response of the infinite treated plate represented by the Fourier series expansion. This approach establishes closed form mathematical solutions that can be use to quickly study the affect of specific properties of the WRC related to the noise control concept. Additionally, dynamic interaction effects such as mass loading, modal coupling, and increased damping are eliminated, thus leaving the pure WRC behavior for investigation.

5.2 Infinite 2D Plate Model

The model consists of an infinite plate with a standing plane bending motion of frequency ω and wavenumber vector k_b, as shown in Figure 5.1.

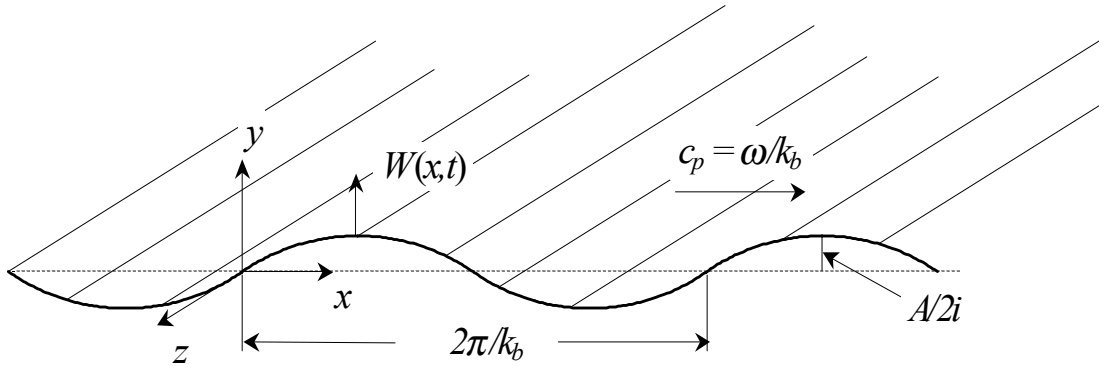

Figure 5.1: Transverse bending wave in infinite plate

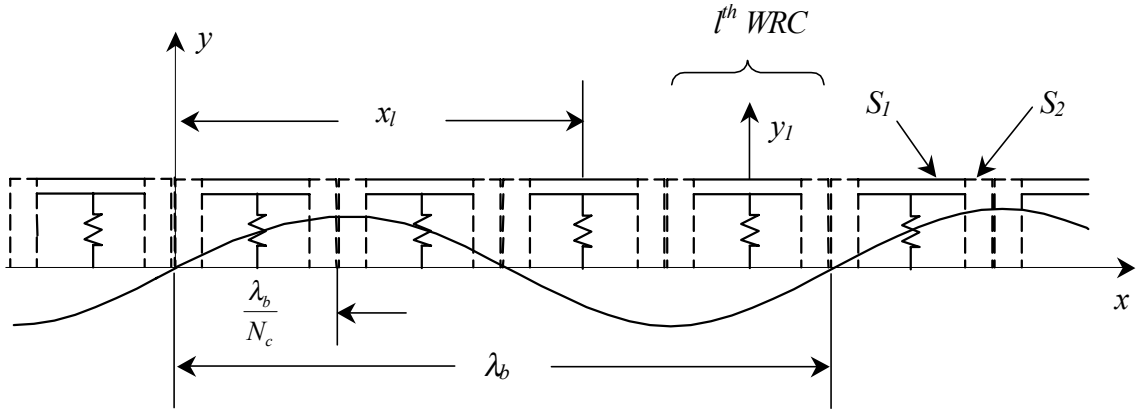

Figure 5.2: Array of identical WRC

The normal displacement at any point on the surface of the plate can be written as two waves traveling in opposite direction with the same wavenumber k_b and equal amplitude. That is,

$$w(x,t) = \frac{-A}{2i} e^{i(\omega t - k_b x)} + \frac{A}{2i} e^{i(\omega t + k_b x)} = A \sin(k_b x) e^{i\omega t} \tag{5.1}$$

where $A/2i$ represents the amplitude of the waves.

Now assume an identical array of WRC's applied to the plate such that an integer number of WRC, N_c, fits within a structural wavelength, $\lambda_b = 2\pi/k_b$, as shown in Figure 5.2. In this model, the WRCs are assumed to have only one degree-of-freedom given by the vertical motion, $y_l(t)$, of the cell's plate. Once again, the WRC has two radiating surfaces S_1 and S_2. The surfaces S_1 and S_2 of the cell are defined in terms of the area ratio $\mu = S_1/S_2$ and the condition $S_1 + S_2 = \lambda_b / N_c$. That is

$$S_2 = \frac{\lambda_b}{N_c(1+\mu)} \text{ and } S_1 = \frac{\mu \lambda_b}{N_c(1+\mu)}. \tag{5.2a,b}$$

The center location of the l^{th} cell is then found to be $x_l = \lambda_b(2l-1)/2N_c$. The surface S_1 has the same response as the plate's response $w(x,t)$ while the motion of surface S_2 is the cell's plate response defined by $y_l(t)$. The dynamics of the WRC's center plate is defined by the plate mass M_l, the spring k_l, that attaches the WRC's plate to the infinite plate, and the infinite plate motion $w(x_l,t)$. The equation of motion for the l^{th} WRC is given as follows

$$M_l \ddot{y}_l + k_l y_l = k_l w(x_l, t). \tag{5.3}$$

Substituting the motion of the plate from Eq 5.1 into Eq 5.2, the response of the cell's plate is written as

$$y_l(t) = \frac{A k_l}{k_l - M_l \omega^2} \sin(k_b x_l) e^{i\omega t}. \tag{5.4}$$

Note that in this model the response of the infinite plate $w(x,t)$ is not affected by the WRCs. Thus, only the cell's behavior is considered in the noise reduction.

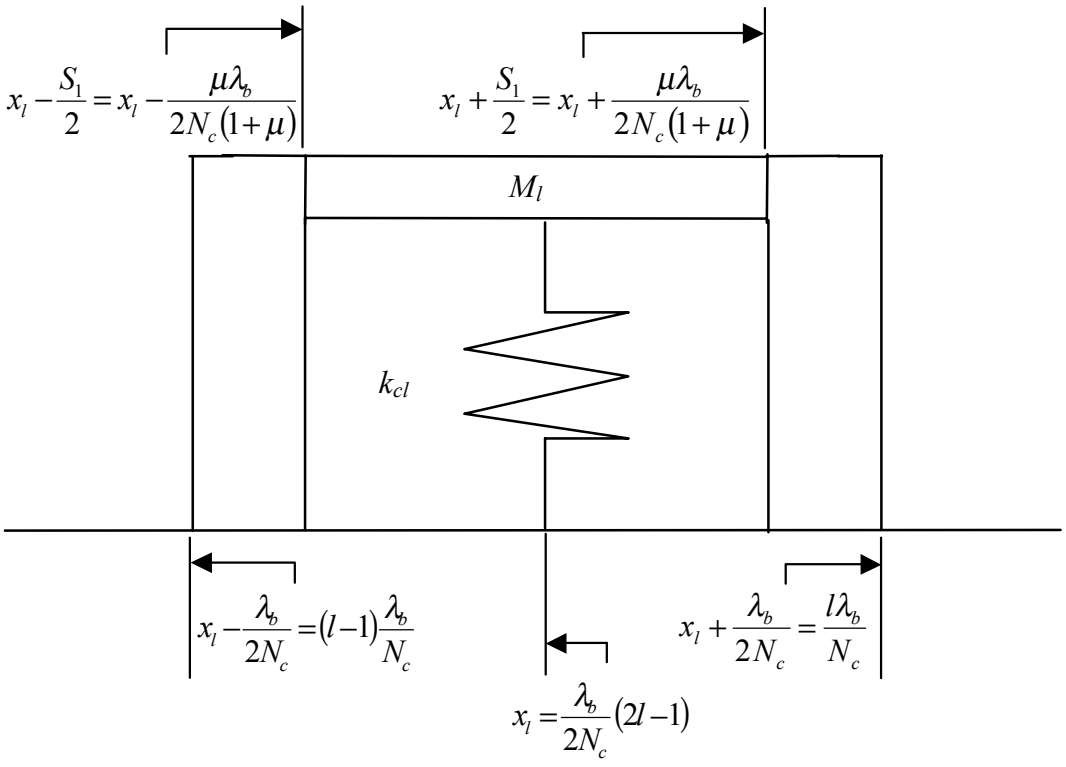

Figure 5.3: WRC dimension boundaries defined in terms of N_c, λ_b, and $\mu=S_1/S_2$.

Using the defined boundary limits shown in Figure 5.3, the response of the treated plate over a structural wavelength is defined as

$$\hat{w}(x,t)=\sum_{l=1}^{N_c}\left\{\left[A\sin(k_b x)e^{i\omega t}\right]\cdot\left[H\left(x-\left((l-1)\frac{\lambda_b}{N_c}\right)\right)-H\left(x-\left(x_l-\frac{\lambda_b\mu}{2N_c(1+\mu)}\right)\right)\right]+\right.$$
$$\left[A\sin(k_b x_l)\frac{k_l}{k_l-M_l\omega^2}e^{i\omega t}\right]\cdot\left[H\left(x-\left(x_l-\frac{\lambda_b\mu}{2N_c(1+\mu)}\right)\right)-H\left(x-\left(x_l+\frac{\lambda_b\mu}{2N_c(1+\mu)}\right)\right)\right]+ \quad (5.5)$$
$$\left.\left[A\sin(k_b x)e^{i\omega t}\right]\cdot\left[H\left(x-\left(x_l+\frac{\lambda_b\mu}{2N_c(1+\mu)}\right)\right)-H\left(x-\left(\frac{l\lambda_b}{N_c}\right)\right)\right]\right\}$$

where $H(.)$ is the Heavy-side function [36]. It is important to remark that to model a WRC with two dofs i.e., translation and rotation, only the second term in Eq 5.5 would require modification to implement the rotational response.

Because of the spatial periodicity of the response with period λ_b, the response in Eq 5.5 can be expressed by Fourier Series expansion as follows

$$\hat{w}(x,t)=\sum_{n=1}^{\infty}b_n\sin(nk_b x)e^{i\omega t}=\sum_{n=1}^{\infty}\frac{-b_n}{2i}\left\{e^{i(\omega t-nk_b x)}-e^{i(\omega t+nk_b x)}\right\} \quad (5.6)$$

where

$$b_n=\frac{2}{\lambda_b}\int_{x=0}^{x=\lambda_b}\hat{w}(x,t)\sin(nk_b x)dx \quad (5.7)$$

are solved in Appendix A.

The response of the plate/WRC system in Eq 5.6 consists of an infinite set of standing waves or two opposite traveling waves with wavenumber nk_b (n = 1, 2, ..., ∞). The fact that the response $\hat{w}(x,t)$ can be expressed in terms of traveling waves allows for all acoustic variables to be written in closed form.

The acoustic pressure is easily computed as the superposition of the pressure due to each propagating wave. That is

$$p(x,y,t)=\sum_{n=1}^{\infty}\left[P_n^{(+)}e^{i\left(wt-nk_bx-k_yy\right)}+P_n^{(-)}e^{i\left(wt+nk_bx-k_yy\right)}\right] \tag{5.8}$$

Where $P_n^{(+)}$ and $P_n^{(-)}$ are the complex amplitude of the pressure wave generated by the positive and negative propagating structural waves. These amplitudes are obtained by using the matching condition at the fluid-structure interface, i.e., $y = 0$ [35]. That condition leads to

$$P_n^{(+)}=P_n^{(-)}=\frac{i\omega\left(b_n/-2i\right)\rho c}{k_y} \tag{5.9}$$

which yields the acoustic pressure field as

$$p(x,y,t)=\sum_{n=1}^{\infty}\frac{i\omega b_n\rho_o c}{k_y}sin\left(nk_bx\right)e^{i(\omega t-k_yy)} \tag{5.10}$$

The y-component of the acoustic wavenumber k_y, is determined from the radiating condition (see Chapter 3.7) as

$$k_y=\begin{cases}\left[k_o^2-\left(nk_b\right)^2\right]^{1/2} & if \quad nk_b<k_o \quad propagating\ wave\\ -i\left[\left(nk_b\right)^2-k_o^2\right]^{1/2} & if \quad nk_b>k_o \quad evanescent\ wave\end{cases} \tag{5.11a,b}$$

The frequency when a wave transitions from subsonic to supersonic is obtained from $k_o=nk_b$, which is referred to as transition frequency. In addition to the sound pressure field, the sound intensity vector field can be easily computed. This vector field is useful to illustrate the acoustic energy flow patterns. To determine the intensity vector, the fluid particle velocity vector is first solved using Euler's equation as

$$-\frac{\partial p}{\partial x}=i\omega\rho_o v_x \text{ and } -\frac{\partial p}{\partial y}=i\omega\rho_o v_y \tag{5.12a,b}$$

where v_x and v_y are the x and y components of the acoustic particle velocity. Replacing Eq 5.10 into Eq 5.12a,b gives

$$v_x = \sum_{n=1}^{\infty} \frac{-nb_n k_b c}{k_y} cos(nk_b x) e^{-ik_y y} \quad \text{and} \tag{5.13a}$$

$$v_y = \sum_{n=1}^{\infty} icb_n \, sin(nk_b x) e^{-ik_y y} \, . \tag{5.13b}$$

The intensity vector components I_x and I_y are then defined as

$$I_x = \frac{1}{2} \mathrm{Re}\left[p v_x^* \right] \text{ and } I_y = \frac{1}{2} \mathrm{Re}\left[p v_y^* \right]. \tag{5.14a,b}$$

Replacing Eqs 5.10 and 5.13 into Eq 5.14 gives

$$I_x(x,y) = \frac{1}{2} Re\left[\sum_{n=1}^{\infty} \frac{i\omega\rho_o c b_n}{k_y} sin(nk_b x) e^{-ik_y y} \sum_{m=1}^{\infty} \frac{-mb_m^* k_b c}{k_y} cos(mk_b x) e^{ik_y y} \right] \text{and} \tag{5.15a}$$

$$I_y(x,y) = \frac{1}{2} Re\left[\sum_{n=1}^{\infty} \frac{i\omega\rho_o c b_n}{k_y} sin(nk_b x) e^{-ik_y y} \sum_{m=1}^{\infty} -icb_m^* \, sin(mk_b x) e^{ik_y y} \right]. \tag{5.15b}$$

The sound intensity at the surface of the treated infinite plate is given as

$$I_y(x,0) = \frac{1}{2} Re\left[\sum_{n=1}^{\infty} \frac{i\omega\rho_o c b_n}{k_y} sin(nk_b x) \sum_{m=1}^{\infty} -i\omega b_m^* \, sin(mk_b x) \right] \tag{5.16}$$

By integrating the intensity over a structural wavelength gives the radiated acoustic power per unit wavelength of the treated system

$$\Pi_t = \int_{x=0}^{x=\lambda_b} \frac{1}{2} \mathrm{Re}\left[\sum_{n=1}^{\infty} \frac{i\omega\rho_o c b_n}{k_y} \sin(nk_b x) \sum_{m=1}^{\infty} -i\omega b_m^* \sin(mk_b x) \right] dx \, . \tag{5.17}$$

Performing the integration and using the orthogonality property of the sine function leads to a closed form solution for the acoustic power as

$$\Pi_t = \frac{1}{2}\left[\sum_{n=1}^{nk_b>k_o} \frac{\pi\omega^3\rho_o b_n^2}{k_y k_b}\right] \tag{5.18}$$

where the summation is only the waves that generate sound, i.e., supersonic waves, $nk_b>k_o$.

As reference, the response of the untreated plate is given as Eq 5.1. Taking the same steps, the radiated sound power per unit wavelength is calculated to be

$$\Pi_{ut} = \frac{1}{2}\left[\frac{\pi\omega^3\rho_o A^2}{k_y k_b}\right]. \tag{5.19}$$

5.3 Infinite 2D Plate Wavenumber Transform Analysis

With the beam and plate-WRC models several dynamic interactions existed which added complexity to the study of the acoustic response. Using the present model the dynamic interactions are eliminated and only the acoustic behavior of the WRC is considered in the computation of the noise reduction. To this end, the infinite wavenumber model is used to study the effect of the weak radiating cell applied as noise treatment per structural wavelength and characterize the fluid motion near the surface of the plate at particular frequencies.

Here the results of 4 WRCs per structural wavelength is presented. The cell's mass and spring stiffness are chosen such that the vertical resonance of the WRC(s) is held at 75 Hz. A loss factor of 8 % is added to the cell's spring constant. The surface area ratio was

selected such that $S_1 = S_2$, (i.e., $\mu = 1$). The structural wavelengths considered are λ_b = 6.28 and 3.38 m over a frequency range of 0-400 Hz.

Figures 5.4 and 5.5 show the sound power spectrum of the untreated plate and the plate treated for the two wavelength cases, respectively. Clearly shown in each figure are the transition frequencies. The results at these frequencies are not valid because finite vibration of the structure results in an infinite pressure, (i.e. $nk_b = k_o$.) As mentioned, this case cannot physically occur in the real world. The true representation of the acoustic response at $nk_b = k_o$ can be modeled by considering the fluid interaction. Although, this is beyond the scope of this thesis, the addition of fluid interaction would allow the study of the WRC in different medium (e.g., water). Above the transition frequency 55 Hz, Figure 5.4 shows an increase in noise of 15.8 dB were the cells pass through their resonance frequency. As the frequency increases, the dipole effect of the cell is also clear with noise attenuation of 21 dB. In Figure 5.5, the cells' resonance (i.e., 75 Hz) is subsonic for k_b = 1.8571, where the transition frequency occurs at 102Hz. The dipole effect appears shortly after at 107 Hz with a 21.8 dB reduction. Using case results from Figure 5.5, sound attenuation at higher frequency during the cell's suppression is estimated at 6.5 dB. From results of both finite beam and plate models as well as experimental results, the estimated increased noise and attenuation of sound power compare well.

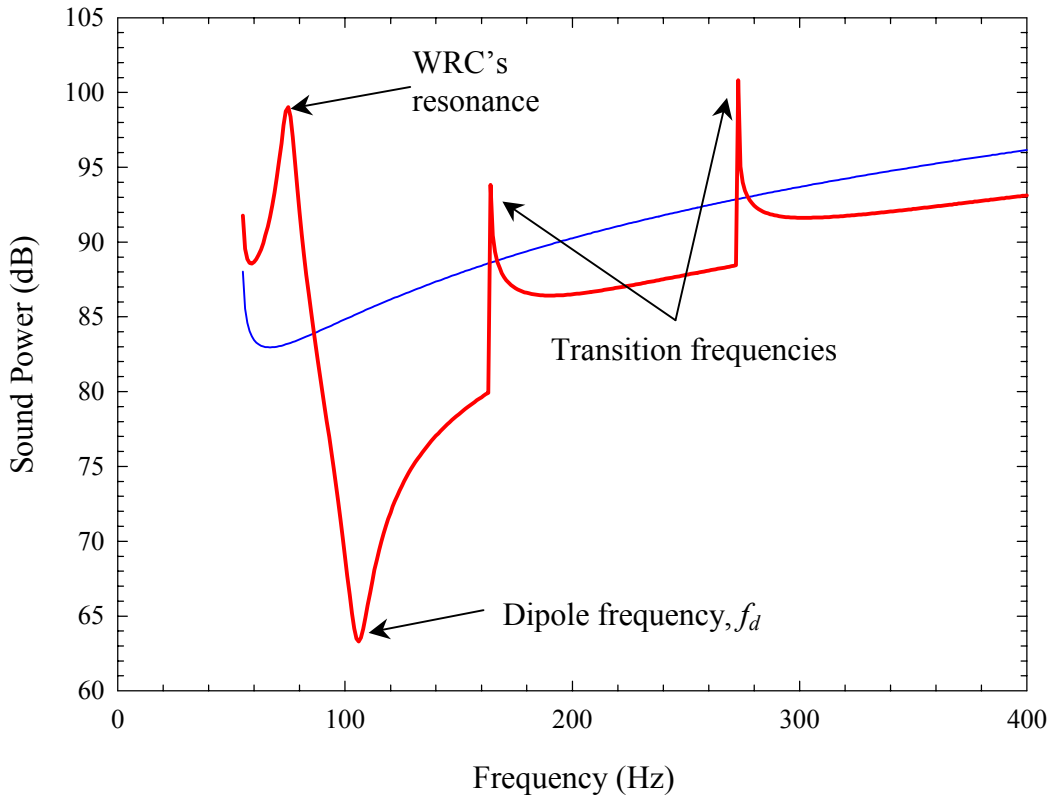

Figure 5.4: Sound Power spectrum for k_b = 1.00 of the untreated plate (——) and the treated plate (——).

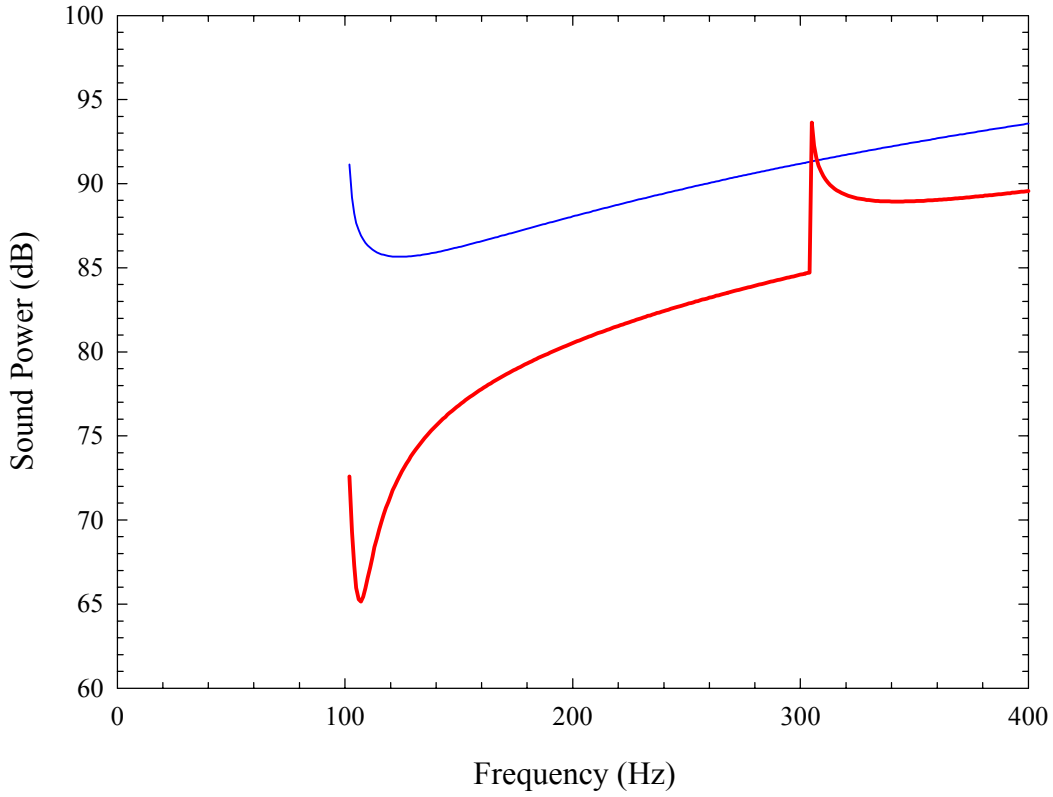

Figure 5.5: Sound Power spectrum for $k_b = 1.8571$ of the untreated plate (——) and the treated plate (——).

In the previous finite beam and plate models, the intensity field was not computed due to computational limits of the codes. However, the intensity vectors are easily computed with the present infinite model. Shown in Figure 5.6 - 5.9 are the intensity vectors plot for the untreated plate and the treated plate at several frequencies. Because of the large range of intensity values, each plot has a different scale that is indicated in the caption of the figures. Figure 5.6 shows the intensity field at 45 Hz, where all traveling waves are subsonic i.e., only evanescent waves are generated in the fluid and do not radiate to the far-field. Figure 5.7 shows the untreated plate intensity field at 105 Hz, which radiates into the far field. Figure 5.8 shows the treated plate at the same frequency with the WRCs operating near the dipole frequency. As expected, the intensity field shows the fluid passed back and forth between the two surfaces, S_1 and S_2. Also noticeable, in this figure, is the presence of evanescent waves, recognized by diminishing intensity vectors magnitude with increased distance from the treated plate. Figure 5.9 show the treated plate at 250 Hz for k_b =1. At this higher frequency, the WRCs have stopped responding to input, as seen in the figure, where intensity vectors from the surface S_2 of the cells' plates are notable smaller than the plate surface S_1. This relates the second method of noise control developed by the WRCs (i.e., suppression of the cell's plate).

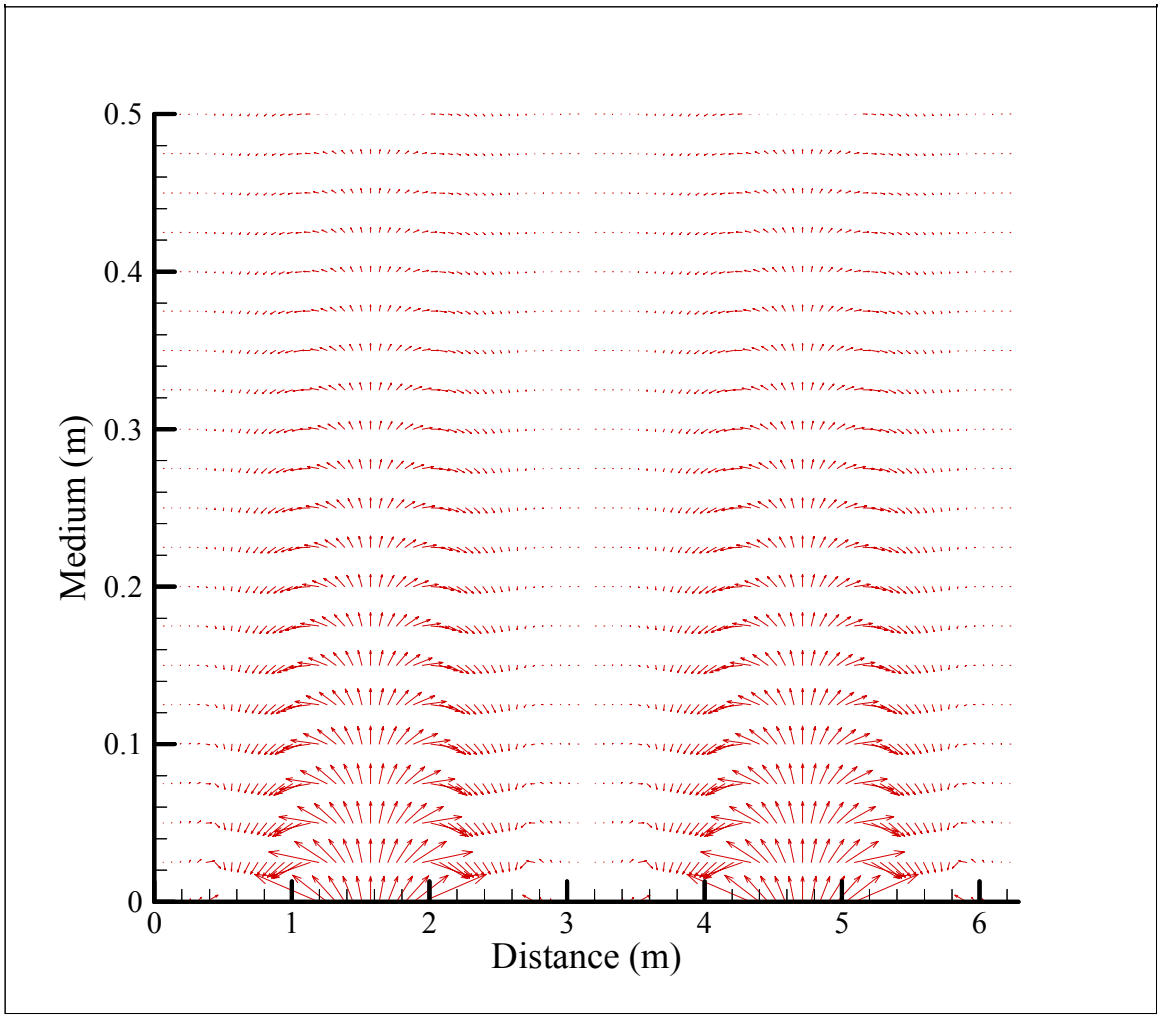

Figure 5.6: Intensity Vectors for k_b = 1.0 and f = 45 Hz with 4 cell as treatment. Scale 50,000,000 cm/(W/m^2)

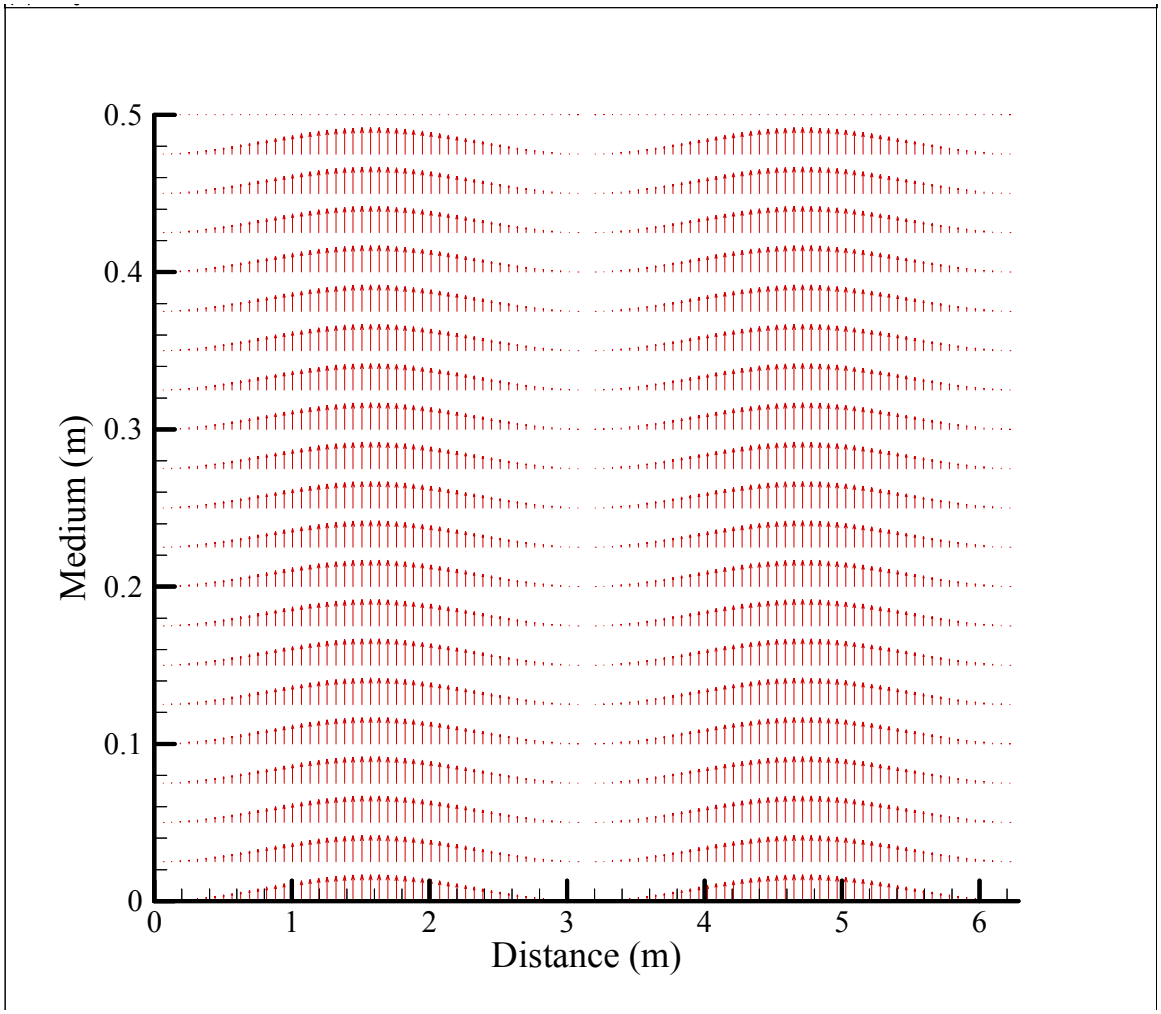

Figure 5.7: Intensity Vectors for k_b = 1.0 and f = 105 Hz of untreated beam. Scale 5000 cm/(W/m^2)

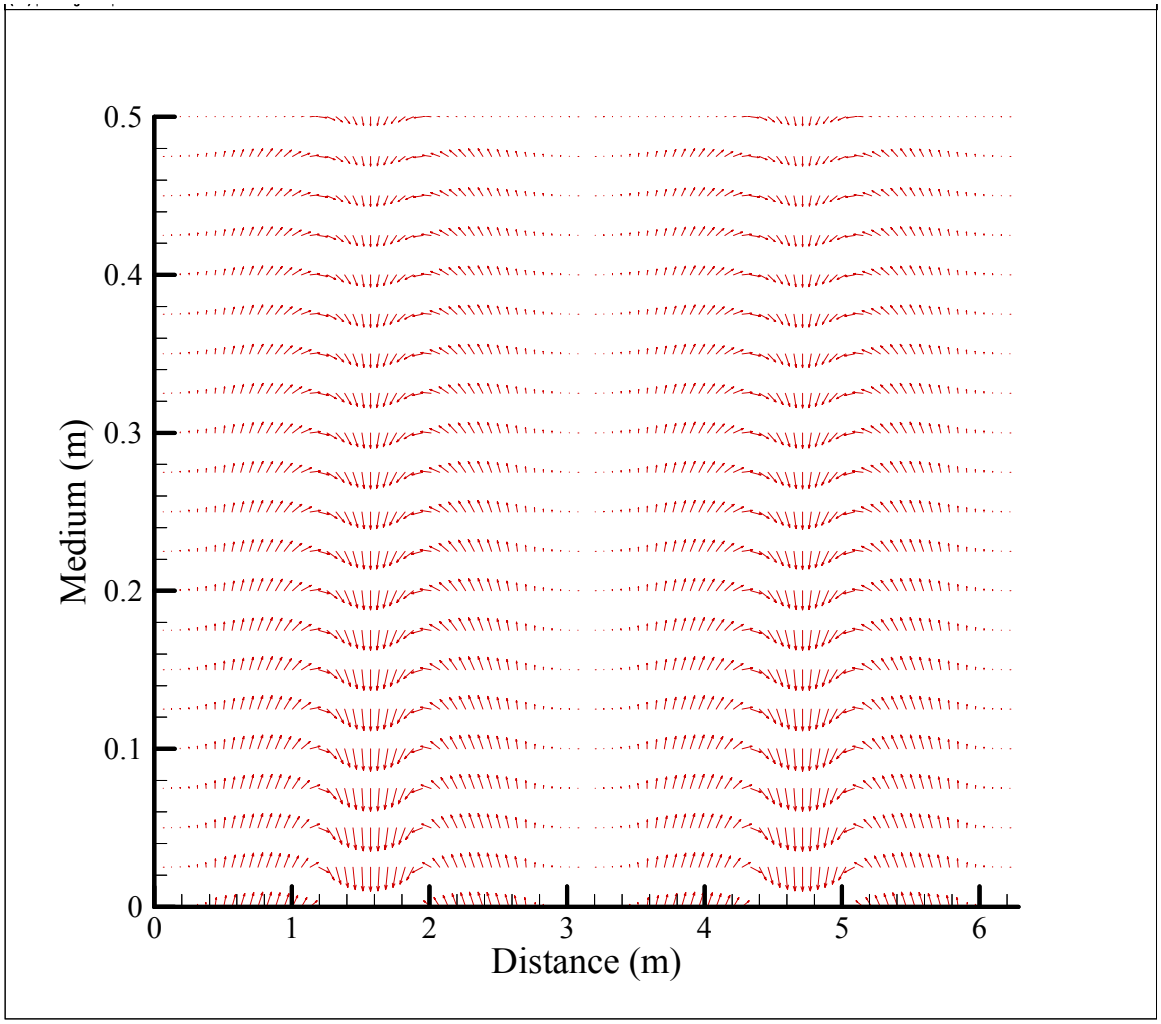

Figure 5.8: Intensity Vectors for k_b = 1.0 and f = 105 Hz with 4 cell as treatment. Scale 80,000 cm/(W/m^2)

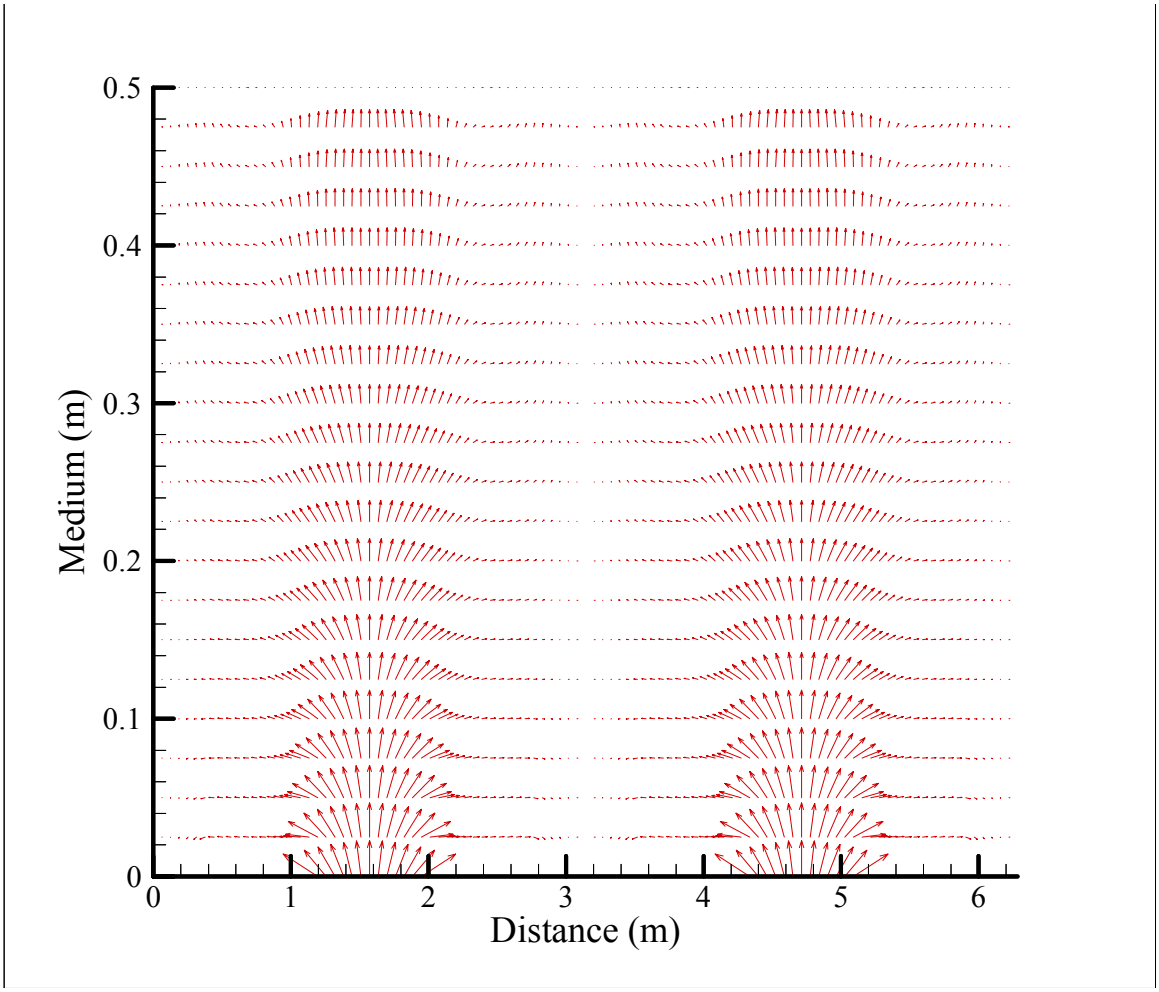

Figure 5.9: Intensity Vectors for k_b = 1.0 and f = 250 Hz with 4 cell as treatment. Scale 1500 cm/(W/m^2)